AIMS Materials Science, 4(6): 1231-1239.
DOI: 10.3934/matersci.2017.6.1231
Received: 24 July 2017
Accepted: 21 November 2017
Published: 29 November 2017

http://www.aimspress.com/journal/Materials

Short review

On the annihilation of dislocation dipoles in metals

Hao Wang *

Institute of Metal Research, Chinese Academy of Sciences, Shenyang 110016, P. R. China

*** Correspondence:** Email: haowang@imr.ac.cn.

Abstract: During plastic deformation, there is a wealth of dislocation reactions, in which dislocation dipoles may play an important role. In this review, first, the history of dislocation dipole annihilation is revisited. Then, recent progresses in elucidating the atomic-scale processes during dipole annihilation are presented with examples from representative systems. Last, the consequence of dipole annihilation, as well as experimental verifications are introduced.

Keywords: plasticity; dislocation; metal; mechanical behavior; annihilation

1. Introduction

As materials are pushed to extremes of temperatures and stresses, they become increasingly sensitive to their internal microstructure. For instance, aero-engine turbines would fail at service temperatures if blades crept beyond certain tolerances. Yet, the strength and plastic deformation of metals and alloys are largely achieved and controlled by linear defects, the dislocations, which carry an elemental distortion, represented by their Burgers vector. The mutual interactions between dislocations or between dislocations and obstacles determine microstructural self-organization and give rise to hardening effects. However, the mechanism of hardening is still “the most difficult remaining problem”, since various hardening theories fail to provide comprehensive explanations to such a phenomenon. Transmission electron microscopy (TEM) observations and dislocation dynamics simulations show that, at the early stage of hardening, there is a wealth of dislocation reactions, where dislocation dipoles may play an important role. But TEM results are limited by resolution and due to the lack of long-range strain field of the dipole, several crucial features were left unattended.

In this review, first, the history of dislocation dipole annihilation is revisited. Then, recent progresses in elucidating the atomic-scale processes during dipole annihilation are presented with

examples from representative systems. Last, the consequence of dipole annihilation, as well as experimental verifications are introduced.

2. History of Dislocation Dipole Annihilation

Dislocation annihilation by cross-slip of screw dislocations and by climb otherwise, plays a key role in recovery processes. Of particular importance is the mutual annihilation of edge dipolar configurations within dislocation entanglements such as walls of persistent slip bands in fatigued samples. The investigation originates from the old question of dislocation patterning discovered in FCC metals associated with the end of stage I and the transition to stage II [1,2], where self-organization under single slip is particularly intriguing since dislocations under interaction then share the same operating Burgers vector. With the origin of such patterning still unclear [3], and with a lack of documentation and direct observations, it is agreed that a substantial number of prismatic loops of finite length exist after the formation of the tangles (e.g., see Refs. [4,5]).

The mechanism of athermal annihilation of edge dipoles was first introduced by Essmann and Rapp [6] to model the experimental strain dependence of the dislocation density in stages I and II of neutron-irradiated Cu (see Figure 1 for a review). This model hypothesizes that below a certain approach distance, defined as the distance between the two glide planes of the approaching dislocations, edge dipolar dislocations annihilate athermally forming invisible debris of almost atomic dimension. Fitted to experimental data, the model leads to a critical dipole height of 1.6 nm (~$7d_{111}$, where d_{111} is the {111} interplanar distance) for spontaneous dipole disintegration. The notion of a minimum dipole height plays a pivotal role in certain models of the plastic strain localization and of the dislocation patterning associated with persistent slip bands in fatigued FCC metals [7,8,9]. In these models, the contribution of the debris resulting from dipole annihilation is merely ignored.

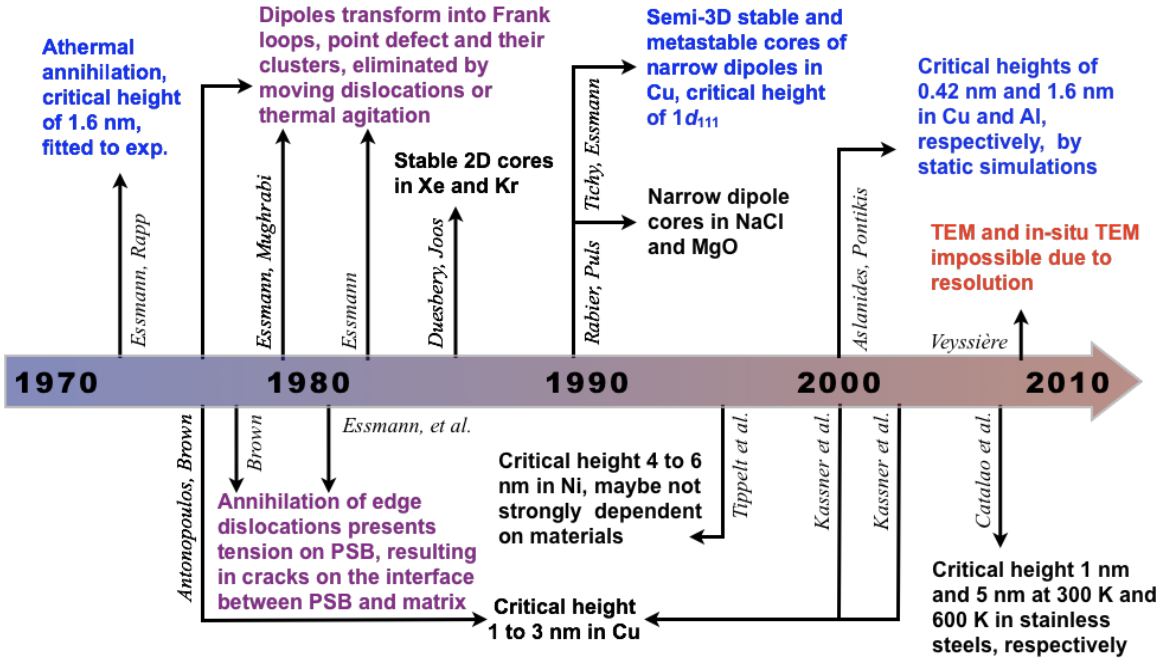

Figure 1. A chronicle of the early investigations on dislocation annihilation.

In an experimental and theoretical analysis conducted in relation with tensile and cyclic deformation tests of Cu, Essmann and Mughrabi were led to postulate that an edge dipole less than 1.6 nm in height transforms into a chain of point defect clusters whose subsequent role in deformation was however not elaborated [7]. Transmission electron microscopy (TEM) studies in Cu concluded to a minimum edge dipole height of about 3 nm, down to 1 nm [4,10,11,12]. Reporting a minimum average dipole height of approximately 4 nm and 6 nm at 77 K and 750 K, respectively in fatigued Ni, Tippelt et al. [13] later confirmed the analysis made in Cu, thus implying that this critical distance is not strongly material dependent. In a similar TEM analysis in AISI 316L stainless steel, Catalao *et al*. claimed critical heights of 1 and 5 nm at 300 K and 900 K, respectively [14]. Recent simulations of TEM images of dipoles of undissociated dislocations, however, revealed that below 5 to 6 nm, dipole heights cannot be measured in practice by the TEM method designed for this purpose, and they showed that the analysis worsens if dissociated dipolar dislocations are to be dealt with [15,16].

In early simulations of dipoles, static relaxation was performed by Duesbery and Joos [17] on Kr and Xe and by Rabier and Puls [18] on NaCl and MgO. However, with the ignorance of point defect diffusion, as well as the strong Coulomb effect in ionic compounds, these results do not have a common sense. For metals, Tichy and Essmann [19] arrived at an annihilation distance of 1*d* much smaller than the commonly accepted critical height of 1.6 nm. This result was somewhat questioned in subsequent numerical simulation [20] that yielded critical heights of 0.42 nm and 1.6 nm for copper and aluminum, respectively. Both computer investigations were, however, carried out on cavities as starting configurations and at 0 K thus including neither thermal vibration nor diffusion. Indeed, there is general agreement that the by-products of dipole annihilation should not just evaporate but their nature has received little attention. In annihilating at finite temperatures, the dipoles are thought to transform either into Frank loops subsequently transformed and swept out by gliding dislocations [19,20], or else into point defects or point defect agglomerates whose properties at a macroscopic scale are for instance manifested by surface extrusions in fatigue-tested Cu [21,22]. There is experimental evidence that nano-sized defects are indeed present in significant densities in the walls of persistent slip bands in fatigued Cu [23,24].

Currently, it is commonly accepted that narrow dislocation dipoles will spontaneously disintegrate. However, the product is believed unimportant during plastic deformation with their evolution almost undocumented. In fact, the stability of narrow dislocation dipoles relates closely to a number of mechanical properties, including the critical annihilation distance [7] and back stress [25,26], and contributes to the localization of deformation through the formation of deformation debris by dipole disintegration [5,27,28]. Dipole annihilation and subsequent point defect evolution not only has atomic-scale importance, but also affect meso-scale models, e.g., dislocation dynamics and constitutive laws. As an example, the discrepancy between elastic and MD predictions on the partial dissociation distance was revealed in Al [29]. Therefore, in the following context, we will review firstly the issue of dipole annihilation in various metals and alloys with face-centered cubic (FCC), body-centered cubic (BCC) and hexagonal close-packed (HCP) lattices; secondly the nature of the atomic-sized debris resulting from dipole annihilation; and lastly dipole-induced strengthening.

3. Recent Progresses

3.1. Athermal and Thermal Annihilation

In a series of recent studies [5,27–32] focusing on the atomic-scale interaction between dipolar dislocations, some new features were revealed regarding both athermal and thermal annihilations. At low temperature without thermal agitation, dipoles spontaneously rearrange. At very small height, 1*d* or 2*d* (*d* is the interplanar distance of the dislocation glide planes), vacancy or interstitial tubes are formed. At intermediate height, i.e., 3*d* to 6*d*, reconstructed cores are formed. Higher than 6*d*, classical vertical or inclined configurations are formed. Note that the above range is materials dependent. At high temperature with thermal agitation, the above configurations gradually transform into vacancy/interstitial clusters, stacking fault tetrahedral, interstitial loops, etc. Athermal and thermal annihilation configurations are exemplified in Figure 2 and Figure 3 for 1*d* to 4*d* edge dipoles in typical FCC, BCC and HCP systems, Cu, Fe and Ti, respectively.

Apart from the above similarity, at both low and high temperature, the atomic structures of the annealed configurations depend strongly on materials, dipole height and orientation. For detailed comparison, please refer to Refs. [28,31]. In general, low temperature stability is mostly relevant to the stacking fault energy, which determines the separation of partial dislocations and affects the mutual interaction of the constitutive dislocations; while high temperature stability is also influenced by vacancy/interstitial migration energy.

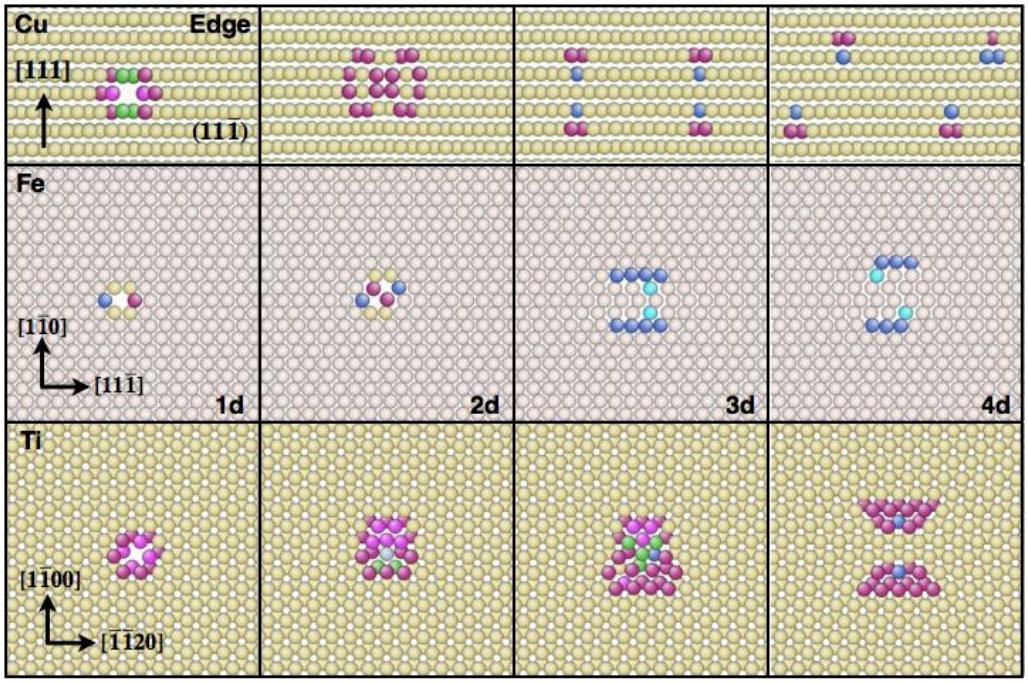

Figure 2. Athermally annihilated configurations of pure edge dipoles in Cu, Fe and Ti after MD annealing at 1 K. Atoms are colored according to their coordination number. Lattice orientations are indicated.

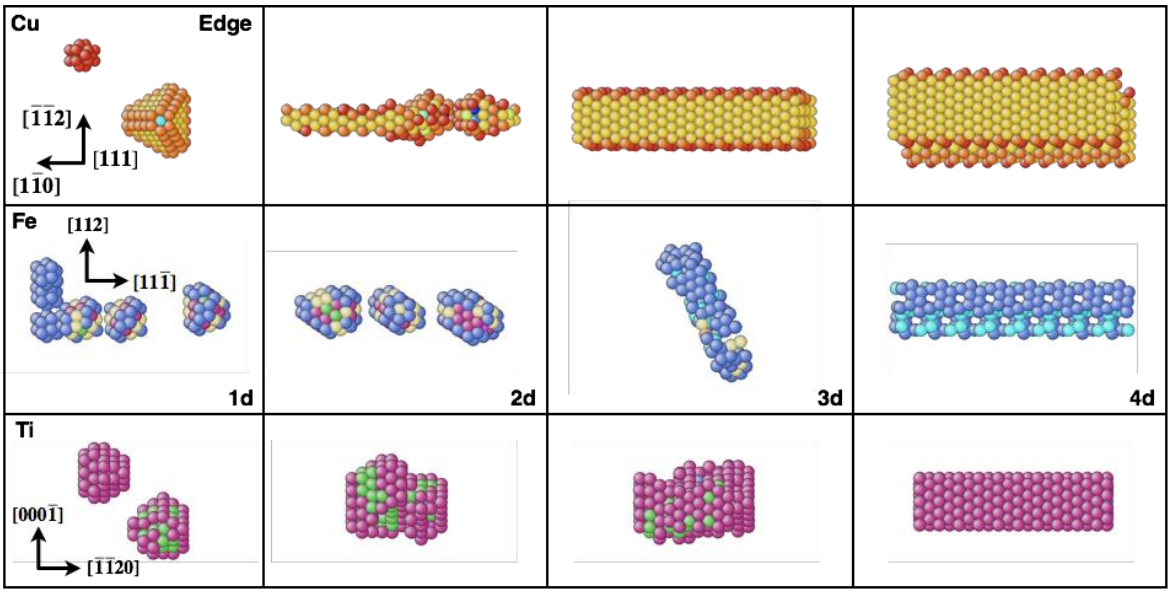

Figure 3. Thermally annihilated configurations of pure edge dipoles in Cu, Fe and Ti after MD annealing for 1 ns at 1300 K, 2300 K and 1700 K, respectively. Atoms are colored according to their FCC-coordination number for Cu to show the stack faults, and otherwise according to their coordination number. Lattice orientations are indicated.

3.2. Defect Formation and Consequence

Some of the annihilation debris are stable against thermal annealing and moreover, as indicated in Refs. [28,30], certain atomic diffusion paths correspond with activation energies significantly lower than bulk diffusion, which indeed accelerates the overall formation processes. Employing saddle-point search methods, activation energies of the atomic processes therein are obtained and the lifetime of the above by-products is estimated, showing the stability of certain clusters and loops on the experimental timescale (for details, see Refs. [31,33,34]). Using objective kinetic Monte Carlo simulations, clustering and its influence on metal properties can also be revealed [33,34]. Among the annihilation debris, interstitial loops may be of interest due to their role during plastic deformation. Atomic simulations have suggested their strengthening effect [35]. A thorough review of debris induced intermittent plastic flow can be found in Ref. [36].

Figure 4 exemplifies the atomic diffusion processes in Al [28] and Ti [31] during annihilation. Local short circuit diffusion operates, transforming the linear dipoles into vacancy or interstitial clusters. Unique diffusion paths, in particular those with activation energies significantly lower than bulk diffusion, were analyzed in FCC systems [30,37] during the initial clustering stage. Stable dipole and debris produce strengthening by locking the constitutive dislocation and interacting with mobile dislocations, respectively. The breaking stress is significantly increased by the formation of stable dipolar configurations [29,38], while in annihilation debris, e.g., interstitial loops, strongly interact with incoming dislocations by forming decoration [35].

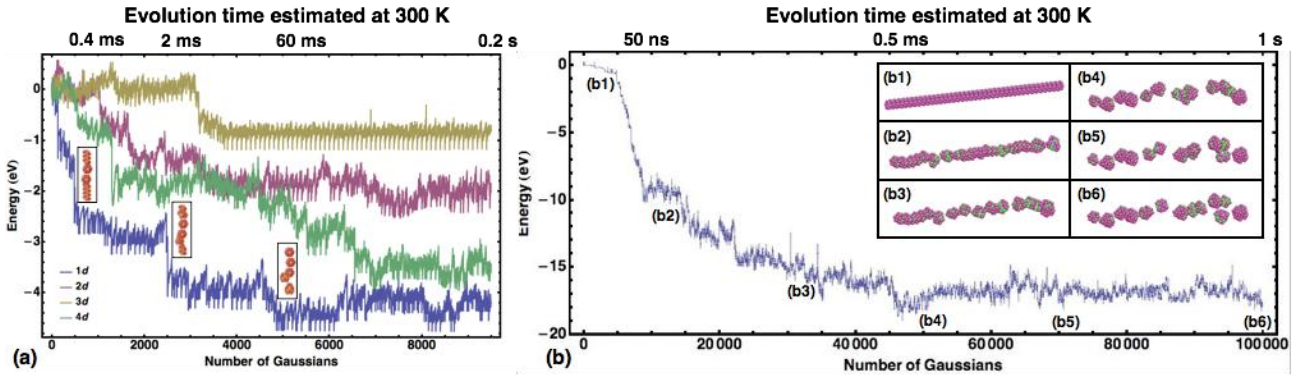

Figure 4. Energy profiles and debris evolution against time at 300 K in Al (a) [28] and Ti (b) [31]. Energy paths were calculated with the autonomous basin climbing (ABC) algorithm [39]. In both (a) and (b), the left axes represent the intantaneous energy of the systems; the bottom and top axes correspond with the number of Gaussians (see Ref. [39] for details) during the ABC calculations and the estimated evolution time at 300 K, respectively. The insets are instataneous atomic configurations at different evolution stages.

3.3. Experimental Verifications

Dipole and debris structures were frequently observed in deformed TiAl alloys by transmission electron microscopy (TEM) [5,40–47]. Most recent high-resolution TEM observations [5] have made good verifications of the above atomic-scale simulations. In a series of experiments on intermetallic TiAl alloys, Appel and coworkers have observed plenty of dipoles in deformed samples. It is thus believed that dipolar interaction and dipole annihilation should be well considered in meso-scale models and constitutive laws to count for their contribution on internal stresses [25,26], dynamic recovery [7] and the temperature retention of strain hardening [5]. In particular for faulted dipoles in TiAl, simulations are in full agreement with experiments in 1) atomistic simulations [38] predicts exactly the same atomic structure as high-resolution TEM observations [5]; and 2) the long-term stability of faulted dipoles indicated by atomistic simulations [38] is consistent with their abundance in deformed samples [45].

4. Conclusion

In summary, despite the long-time investigation on dipole annihilation, there are still several key questions remain unanswered. Recently, narrow dislocation dipoles have been systematically investigated with atomistic simulations and high-resolution experiments. The atomic structures of narrow dipolar configurations, their formation energies and the activation energies during their evolution were determined. The atomic-scale structure and long-term stability of faulted dipoles are in full agreement with high-resolution and ordinary TEM observations. This indicates the importance of incorporating dipole effects in the various models of predicting mechanical properties.

Acknowledgements

This work is supported by the National Key Research and Development Program of China (2016YFB0701304), the Natural Science Foundation of China (51671195) and the Youth Innovation Promotion Association of Chinese Academy of Sciences (2015151). HW is grateful to Dr. Patrick Veyssière (1947–2011), Dr. Dongsheng Xu, Dr. David Rodney, Dr. Fritz Appel, Dr. Yunzhi Wang, Dr. Ju Li for fruitful discussions.

Conflict of Interest

There's no conflict of interest.

References

1. Mitchell TE (1964) Dislocations and plasticity in single crystals of face-centred cubic metals and alloys. *Prog Appl Mater Res* 6: 117–237.
2. Veyssière P, Wang H, Xu DS, et al. (2009) Local dislocation reactions, self-organization and hardening in single slip. *IOP Conf Ser: Mater Sci Eng* 3: 012018.
3. Kubin L, Kratochvíl J (2000) Elastic model for the sweeping of dipolar loops. *Philos Mag A* 80: 201–218.
4. Tippelt B (1996) Influence of temperature on microstructural parameters of cyclically deformed nickel single crystals. *Phil Mag Lett* 74: 161–166.
5. Appel F, Herrmann D, Fischer FD, et al. (2013) Role of vacancies in work hardening and fatigue of TiAl alloys. *Int J Plasticity* 42: 83–100.
6. Essmann U, Rapp M (1973) Slip in copper crystals following weak neutron bombardment. *Acta Metall* 21: 1305–1317.
7. Essmann U, Mughrabi H (1979) Annihilation of dislocations during tensile and cyclic deformation and limits of dislocation densities. *Philos Mag A* 40: 731–756.
8. Hahner P (1996) The dynamics of dislocation dipoles during single glide. *Scripta Mater* 34: 435–441.
9. Hahner P, Tippelt B, Holste C (1998) On the dislocation dynamics of persistent slip bands in cyclically deformed f.c.c. metals. *Acta Mater* 46: 5073–5084.
10. Antonopoulos JG, Brown LM, Winter AT (1976) Vacancy dipoles in fatigued copper. *Philos Mag* 34: 549–563.
11. Kassner ME, Perez-Prado MT, Vecchio KS, et al. (2000) Determination of internal stresses in cyclically deformed copper single crystals using convergent-beam electron diffraction and dislocation dipole separation measurements. *Acta Mater* 48: 4247–4254.
12. Kassner ME, Wall MA, Delos-Reyes MA (2001) Primary and secondary dislocation dipole heights in cyclically deformed copper single crystals. *Mater Sci Eng A* 317: 28–31.
13. Tippelt B, Bretschneider J, Holste C (1997) The dislocation microstructure of cyclically deformed nickel single crystals at different temperatures. *Phys Status Solidi A* 163: 11–26.
14. Catalao S, Feaugas X, Pilvin P, et al. (2005) Dipole heights in cyclically deformed polycrystalline AISI 316L stainless steel. *Mater Sci Eng A* 400–401: 349–352.

15. Veyssière P (2006) The weak-beam technique applied to the analysis of materials properties. *J Mater Sci* 41: 2691–2702.
16. Veyssière P, Chiu YL, Niewczas M (2006) Dislocation micromechanisms under single slip conditions. *Z Metallkd* 97: 189–199.
17. Duesbery MS, Joos B (1986) Dislocations in two dimensions I. Floating systems. *Philos Mag A* 54: 145–163.
18. Rabier J, Puls MP (1989) On the core structures of edge dislocations in NaCl and MgO. Consequences for the core configurations of dislocation dipoles. *Philos Mag A* 59: 821–842.
19. Tichy G, Essmann U (1989) Modelling of edge dislocation dipoles in face-centred-cubic lattices. *Philos Mag B* 60: 503–512.
20. Aslanides A, Pontikis V (2000) Numerical study of the athermal annihilation of edge-dislocation dipoles. *Philos Mag A* 80: 2337–2353.
21. Essmann U (1982) Irreversibility of cyclic slip in persistent slip bands of fatigued pure fcc metals. *Philos Mag A* 45: 171–190.
22. Essmann U, Gösele U, Mughrabi H (1981) A model of extrusions and intrusions in fatigued metals I. Point-defect production and the growth of extrusions. *Philos Mag A* 44: 405–426.
23. Antonopoulos JG, Winter AT (1976) Weak-beam study of dislocation structures in fatigued copper. *Philos Mag* 33: 87–95.
24. Piqueras J, Grosskreutz JC, Frank W (1972) The influence of point defect clusters on fatigue hardening of copper single crystals. *Phys Status Solidi A* 11: 567–580.
25. Veyssière P, Chiu YL (2007) Equilibrium and passing properties of dislocation dipoles. *Philos Mag* 87: 3351–3372.
26. Hoppe R, Appel F (2014) Deformation-induced internal stresses in multiphase titanium aluminide alloys. *Acta Mater* 64: 169–178.
27. Wang H, Xu DS, Yang R, et al. (2009) The transformation of narrow dislocation dipoles in selected fcc metals and in γ-TiAl. *Acta Mater* 57: 3725–3737.
28. Wang H, Xu DS, Rodney D, et al. (2013) Atomistic investigation of the annihilation of non-screw dislocation dipoles in Al, Cu, Ni and γ-TiAl. *Model Simul Mater Sc* 21: 025002.
29. Wang H, Xu DS, Yang R, et al. (2008) The transformation of edge dislocation dipoles in aluminium. *Acta Mater* 56: 4608–4620.
30. Wang H, Xu DS, Yang R, et al. (2011) The formation of stacking fault tetrahedra in Al and Cu: I. Dipole annihilation and the nucleation stage. *Acta Mater* 59: 1–9.
31. Wang H, Xu DS, Yang R (2014) Defect clustering upon dislocation annihilation in α-titanium and α-zirconium with hexagonal close-packed structure. *Model Simul Mater Sc* 22: 085004.
32. Brinckmann S, Sivanesapillai R, Hartmaier A (2011) On the formation of vacancies by edge dislocation dipole annihilation in fatigued copper. *Int J Fatigue* 33: 1369–1375.
33. Wang H, Rodney D, Xu D, et al. (2011) Pentavacancy as the key nucleus for vacancy clustering in aluminum. *Phys Rev B* 84: 220103(R).
34. Wang H, Rodney D, Xu DS, et al. (2013) Defect kinetics on experimental timescales using atomistic simulations. *Philos Mag* 93: 186–202.
35. Wang H, Xu DS, Veyssière P, et al. (2013) Interstitial loop strengthening upon deformation in aluminum via molecular dynamics simulations. *Acta Mater* 61: 3499–3508.
36. Niewczas M (2014) Intermittent plastic flow of single crystals: central problems in plasticity: a review. *Mater Sci Tech-Lond* 30: 739–757.

37. Wang H, Xu DS, Yang R, et al. (2011) The formation of stacking fault tetrahedra in Al and Cu: II. SFT growth by successive absorption of vacancies generated by dipole annihilation. *Acta Mater* 59: 10–18.
38. He Y, Liu Z, Zhou G, et al. (2018) Dislocation dipole-induced strengthening in intermetallic TiAl. *Scripta Mater* 143: 98–102.
39. Fan Y, Kushima A, Yildiz B (2010) Unfaulting mechanism of trapped self-interstitial atom clusters in bcc Fe: A kinetic study based on the potential energy landscape. *Phys Rev B* 81: 104102.
40. Zhang YG, Xu Q, Li HX (1992) Observations and formation mechanism of 1/3<121> type faulted dipoles in TiAl deformed at room temperature. *Scripta Metall Mater* 26: 865–870.
41. Viguier B, Hemker KJ, Schaublin R, et al. (1993) Characterizing Faulted Dipoles in TiAl with Electron-Microscopy and Computed Image Simulations. *J Phys IV France* 3: C7-441–C7-444.
42. Xu Q, Zhang YG, Jones IP, et al. (1995) Further verification of 1/3<121> type faulted dipoles in TiAl. *Scripta Metall Mater* 32: 225–228.
43. Gao Y, Zhu J, Cai QG (1995) The observation on faulted dipoles in deformed TiAl-based alloys, in: Horton JA, Baker I, Hanada S, et al., *High-Temperature Ordered Intermetallic Alloys VI*, Pittsbugh, PA: Materials Research Society, 617–622.
44. Viguier B, Hemker KJ (1996) Characterizing faulted dipoles in deformed gamma TiAl. *Philos Mag A* 73: 575–599.
45. Grégori F, Veyssière P (2000) Properties of <011]{111} slip in Al-rich γ-TiAl II. The formation of faulted dipoles. *Philos Mag A* 80: 2933–2955.
46. Chiu YL, Inui H, Nakano T, et al. (2003) The dependence of the faulted dipole density on load orientation in γ-TiAl. *Phil Mag Lett* 83: 485–493.
47. Chiu YL, Gregori F, Nakano T, et al. (2003) The nucleation of faulted dipoles at intersection jogs in γ-TiAl. *Philos Mag* 83: 1347–1363.

AIMS Press